Improving Short-Term QPFs over Complex Terrain with a WRF-LETKF Radar Data Assimilation System: OSSEs on Typhoon Morakot (2009)

Chih-Chien Tsai, Shu-Chih Yang, and Yu-Chieng Liou
Department of Atmospheric Sciences, National Central University, Taiwan

1. Introduction

This study implements a Doppler radar observation operator for the WRF-LETKF data assimilation system (Yang et al. 2012). OSSEs on Typhoon Morakot (2009) are performed to investigate the multivariate interactions in this system with a goal to optimize the assimilation strategies for improving the short-term QPF over complex terrain.

2. Methodology

- LETKF: Local Ensemble Transform Kalman Filter (Hunt et al. 2007)
  1) Simultaneously update the ensemble mean (state) and perturbations (uncertainty) locally in space by

$$\bar{\mathbf{x}}_a = \bar{\mathbf{x}}_f + \mathbf{X}_f\tilde{\mathbf{P}}_a\mathbf{Y}_f^T\mathbf{R}^{-1}(\mathbf{y}_o - \bar{\mathbf{y}}_f)$$

$$\mathbf{X}_a = \mathbf{X}_f\left[(K-1)\tilde{\mathbf{P}}_a\right]^{1/2}$$

$$\tilde{\mathbf{P}}_a = \left[(K-1)\mathbf{I}/\rho + \mathbf{Y}_f^T\mathbf{R}^{-1}\mathbf{Y}_f\right]^{-1}$$

  $\bar{\mathbf{x}}, \mathbf{X}$: ensemble mean and perturbations
  $\bar{\mathbf{y}}, \mathbf{Y}$: ensemble mean and perturbations in the observation space
  $\mathbf{R}$: observation error covariance matrix
  $\mathbf{y}_o$: observations K : ensemble size
  ρ : covariance inflation factor

  2) Grid points can be processed in parallel for computational efficiency.
- Model setup:
  1) Model: WRF-ARW V3.2.1
  2) Physics:
     a) Purdue Lin microphysics
     b) Kain-Fritsch cumulus parameterization
     c) Noah land-surface model
     d) YSU planetary boundary layer
  3) IC and BC: NCEP 1° × 1° FNL

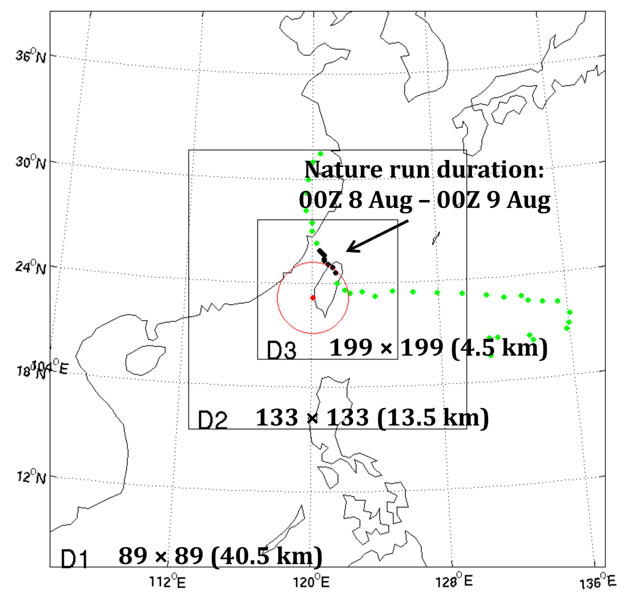

Fig. 1. Simulation domains. The green and black dots mark the best track of Typhoon Morakot (2009). The red dot and circle are the location and coverage of the CWB RCCG S-band Doppler radar.

- Radar observation operator:
  1) Spatial conversion:
     a) Vertical interpolation to the intersections of the sweeps and grid columns
     b) Consider the earth surface curvature, atmospheric refraction and terrain
  2) Variable conversion:
     a) Radial velocity: $V_r = [ux + vy + (w - v_t)z](x^2 + y^2 + z^2)^{1/2}$
        where $v_t = 5.40(p_0/\bar{p})^{0.4}(\rho_a q_r)^{0.125}$ (Sun and Crook 1997)
     b) Reflectivity: $Z_h = 43.1 + 17.5\log(\rho_a q_r)$ (Sun and Crook 1997)

  Z_h is modified to 0 dBZ if negative, where V_r is not available

3. Experimental design

- Simulated nature run and radar observations:
  1) Nature run: 00Z 8 Aug – 00Z 9 Aug
     a) Realistic rainfall compared with CWB observations
     b) Rainbands comprising individual convective cells are well simulated
     c) Windward slopes → rain from the sea + terrain-induced convections
        Lee side → drier downdrafts and less rainfall
     d) Rainband evolution explains the analogous patterns of rainfall
  2) Observations: CWB RCCG radar
     a) Realistic configurations → 7.5-min period, 9 sweeps, 230-km range
     b) Simultaneous observations
     c) Observation errors → 1 m s^{-1} for V_r and 2 dBZ for Z_h
- Assimilation experiments
  1) Perfect model assumption
  2) Data assimilation is performed in the 3rd (finest) domain
  3) Assimilation run:
     a) 12Z 8 Aug → initialized and perturbed into a 30-member ensemble
     b) 12-18Z 8 Aug → model spin-up + assimilation cycles
     c) 18Z 8 Aug - 00Z 9 Aug → deterministic forecast

Table 1. Assimilation strategies.

Name	Assimilation duration	Cycle period	Superobservation-to-grid ratio	Model variables updated by V_r	Model variables updated by Z_h	Assimilation of zero Z_h
CTRL	~ 2 hours	7.5 min	1/4	u, v, w, q_r	q_r	Yes

optimal

References and acknowledgement

Hunt, B. R., E. J. Kostelich, and I. Szunyogh, 2007: Efficient data assimilation for spatiotemporal chaos: a local ensemble transform Kalman filter. *Physica D*, **230**, 112-126.
Sun, J., and N. A. Crook, 1997: Dynamical and microphysical retrieval from Doppler radar observations using a cloud model and its adjoint. Part I: Model development and simulated data experiments. *J. Atmos. Sci.*, **54**, 1642–1661.
Yang, S.-C., E. Kalnay and T. Miyoshi, 2012: Improving EnKF spin-up for typhoon assimilation and prediction. *Wea. Forecasting*, in press.

We are very grateful to Prof. T. Miyoshi and Dr. K.-S. Chung for valuable discussions.
This study is sponsored by Taiwan NSC Grand No. 100-2625-M-008-002.

4. Results and discussions

- Single-point assimilation: P and Q (Fig. 4) are located to the due west and due north of the radar. They contain the most complete u and v information, respectively.
  1) Corresponding fields are broadly corrected
  2) Patterns of w and q_r are noisier than u and v → scale difference
  3) P is better than Q for its higher signal-to-noise ratio (more trustworthy)

  $SNR_P = \frac{-42.7}{1}$ $SNR_Q = \frac{7.4}{1}$

  Radar location is important for effectively observing the wind information

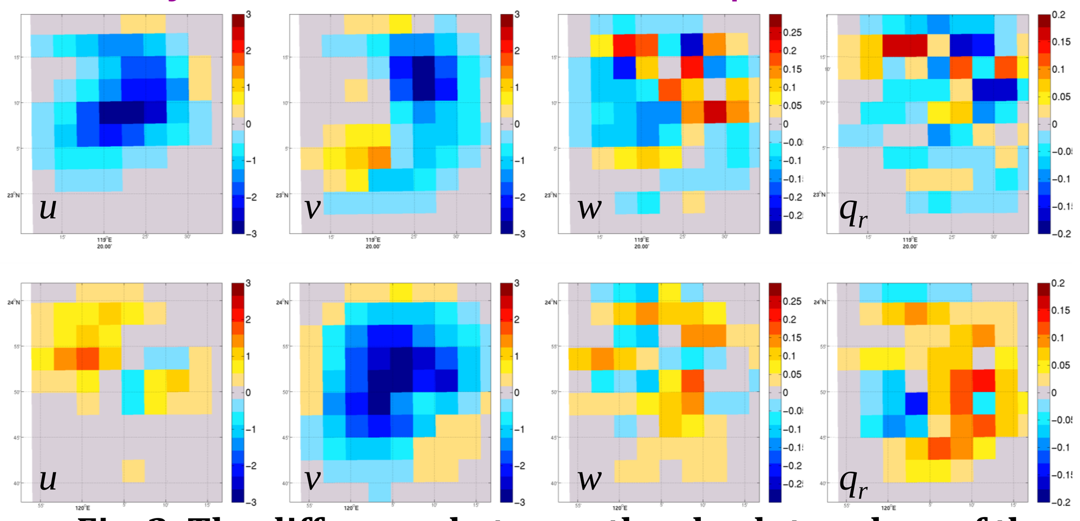

Fig. 2. The difference between the absolute values of the analysis and forecast errors in u, v, w (m s^{-1}) and q_r (g kg^{-1}) (left to right) at z=1 km when assimilating V_r at P and Q (top to bottom). The negative value (blue) represents improvement after assimilation while the positive value (red) represents degradation.

- Assimilation cycles:
  1) Updated model variables:
     V_r → u, v, w and q_r
     Z_h → q_r
  2) Other variables also improve as the model integrates
  3) RMS error and ensemble spread approach, although their trends are dominated by the large-scale dynamics that drives experiment NoDA

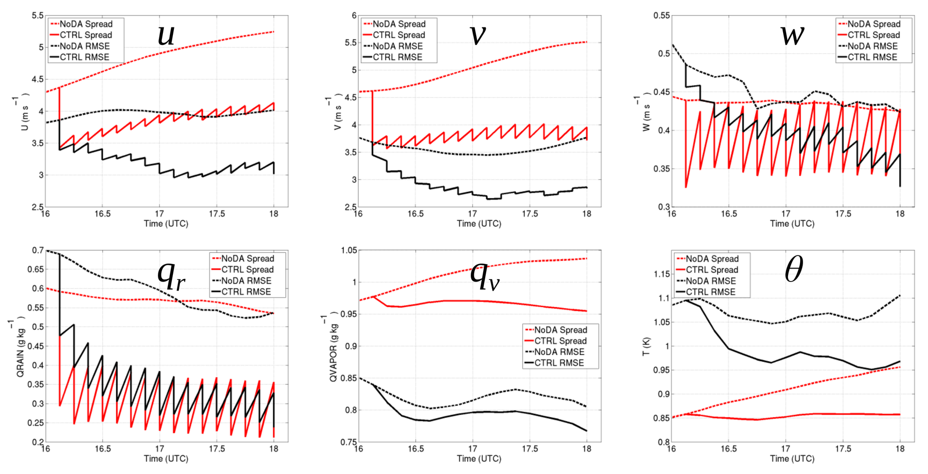

Fig. 3. RMS error (black) and ensemble spread (red) during assimilation cycles for u, v, w (top row; left to right), q_r, q_v and θ (bottom row; left to right) averaged within radar coverage. The solid and dashed lines are of CTRL and NoDA, respectively.

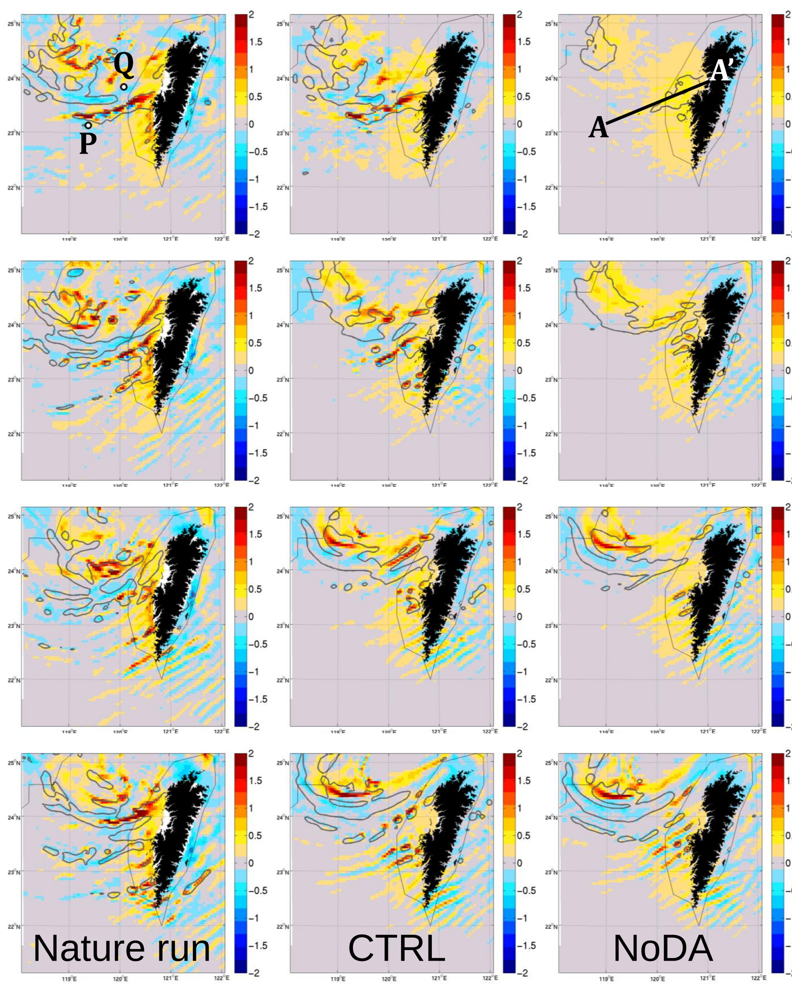

Fig. 4. Hourly maps of w (m s^{-1}; colored) and the contours of q_r=1 g kg^{-1} (gray lines) at z=1 km from 18Z to 21Z 8 Aug (top to bottom) for the nature run, CTRL and NoDA (left to right). P and Q mark the discussed single-point observations.

- Deterministic forecast:
  1) CTRL analysis at 18Z successfully retrieves the intensity and spatial pattern of the spiral rainbands, which are blurred in NoDA
  2) Decaying capability to forecast the rainbands forming later than 18Z
  3) QPF: (Fig. 5)
     a) Both magnitude and pattern are improved for 3 hours, no matter in total or only torrential rain
     b) 3-hour improvement is fair due to the speed of the westerly

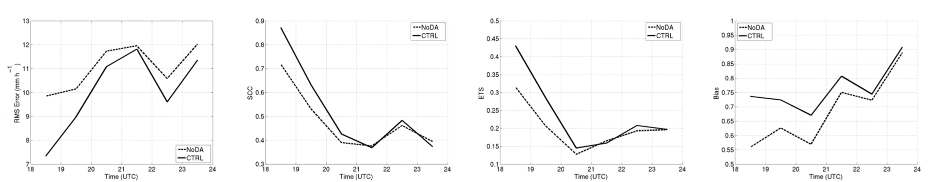

Fig. 5. RMS error, spatial correlation coefficient, ETS and BIAS (above 14.6 mm h^{-1}; CWB's extremely torrential rain alert) of the hourly QPF within radar coverage (left to right). The solid and dashed lines are of CTRL and NoDA, respectively.

- Horizontal localization test:
  1) The CTRL forecast catches better intensity and position of the cell over terrain
  2) The forecast with doubled horizontal localization has a spurious cell over the sea

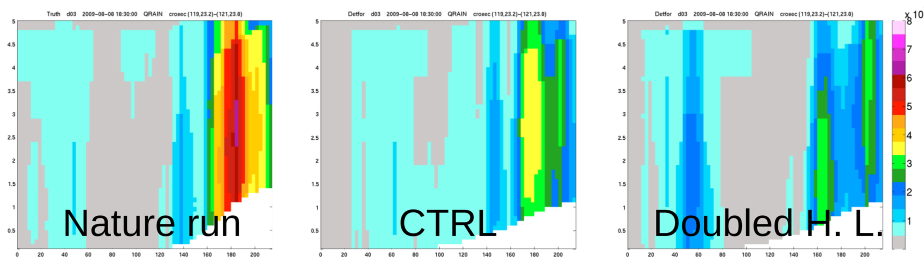

Fig. 6. Vertical cross sections of q_r (kg kg^{-1}) at AA' (see Fig. 4) at 18:30 UTC 8 Aug. From left to right are the nature run, CTRL forecast and the forecast with doubled horizontal localization.

5. Summary and future prospects

- Summary:
  1) In OSSEs on Typhoon Morakot (2009), the WRF-LETKF radar data assimilation system improves the magnitude and pattern of the short-term QPF over complex terrain for 3 hours
  2) Sensitivity tests are performed to optimize the assimilation strategies
  3) Radar location is important for effective observations
  4) Dynamics at large scales (beyond radar coverage) decides the trend
- Future prospects:
  1) Performance in probabilistic QPF by stochastic (ensemble) forecasts
  2) Tasks about real-case studies:
     a) Higher grid resolution
     b) Reflectivity operator considering ice
     c) Radar data quality control
     d) Adaptive inflation and localization